

SUPPRESSION OF CUP-BURNER FLAMES

Fumiaki Takahashi

National Center for Microgravity Research on Fluids and Combustion
NASA Glenn Research Center
Cleveland, OH 44135

Gregory T. Linteris

Fire Research Division, National Institute of Standards and Technology
Gaithersburg, MD 20899

Viswanath R. Katta

Innovative Scientific Solutions Inc.
Dayton, OH 45440

ABSTRACT

The unsteady suppression process of a laminar methane-air co-flow diffusion flame formed on a cup burner has been studied experimentally and numerically in normal earth gravity. The computation uses a time-dependent direct numerical simulation with detailed chemistry. A fire-extinguishing agent (CO_2 or CF_3H) was introduced into a coflowing oxidizer stream by gradually replacing the air (the standard method) or the nitrogen in the air (the constant oxygen concentration method). The agent concentration required for extinguishment was constant over a wide range of the oxidizer velocity, showing a so-called “plateau region.” The measured extinguishing volume fractions of the agents were: CO_2 replacing air, $(15.9 \pm 0.6) \%$; CF_3H replacing air, $(11.7 \pm 0.8) \%$; CO_2 replacing N_2 , $(40.2 \pm 2.0) \%$; and CF_3H replacing N_2 , $(20.3 \pm 1.5) \%$. The cup-burner flame without agent flickered at ~ 11 Hz or ~ 15 Hz, depending on the oxidizer velocity. The flame base sometimes oscillated at half the flickering frequency just before the flame blew off. The suppression of cup-burner flames occurred via a blowoff process (in which the flame base drifts downstream) rather than the global extinction phenomenon typical of counterflow diffusion flames. The numerical simulations predicted the suppression limits and the flickering frequency with good agreements with the experimental observations and, more importantly, revealed the detailed mechanisms of the flame-base oscillation and subsequent blowoff phenomena.

INTRODUCTION

The industry-standard [1] cup burner apparatus is the most widely used [2-12] test for fire-extinguishing agent effectiveness in fire safety engineering. The cup-burner flame is a laminar co-flow diffusion flame with a circular fuel source (2.8 cm diameter, either a liquid pool or a low-velocity gas jet) inside a co-axial chimney with an oxidizer flow. An agent is generally introduced into the coflowing oxidizer in the cup-burner system to determine the critical agent concentration at extinguishment. The cup-burner flame resembles a real fire, which consists of flame segments subjected to various strain rates, including stabilized (or spreading) edge diffusion flames, and exhibits flame flickering (and separation) in normal earth gravity, affecting the air and agent entrainment into the flame zone. Thus, the cup burner flame serves as a scale

model of real fires for evaluating the agent effectiveness. Because of its resemblance to fires, great faith has been placed in agent extinguishment concentrations determined in the cup burner experiment, and many safety codes and design practices are based on the cup-burner values [1]. However, there exists virtually no fundamental understanding of the flame suppression process for this device. Little is known concerning the amount of agent that is transported into various regions of the flame, or whether the extinction occurs globally over the flame or in stabilization regions. Clearly, the understanding of fire suppression by chemical inhibitors as well as inert agents would be greatly improved if their effect in cup-burner flames was investigated from a fundamental perspective.

On the other hand, the counterflow diffusion flames [13] have long been used for studying the flame structure and extinction limits [14-18] because their simple geometries facilitate analytical modeling and the fluid mechanic parameter, i.e., the strain rate, can easily be controlled. Although the critical agent mole fraction at extinction is a function of the strain rate, the cup-burner results generally agree well with the counterflow diffusion flame data for relatively low values of the global strain rate ($a = 2U/L = 50$ to 60 s^{-1} where U = the oxidizer exit velocity and L = the separation distance between the liquid pool surface and the oxidizer duct exit) [15, 16, 19].

Fire-extinguishing agents act to suppress the flame physically and/or chemically [4]. Examples of physically acting agents are carbon dioxide (CO_2) and water-based foam used in the International Space Station and numerous terrestrial applications. These agents are relatively inefficient as fire suppressants [20, 21]. The chemically acting agent, halon 1301 (CF_3Br), which is still used in the Space Shuttle, is highly effective, but its production was banned by the Montreal Protocol in 1995 [22, 23]. Although the existing systems may continue to be used, new agents or techniques are ultimately needed for long-duration missions [21, 24].

As a result of significant progresses in the development of detailed combustion reaction mechanisms and computer technologies over the last decade or two, it is now feasible to simulate various transient combustion phenomena in simple configurations (burner geometry, flow, and fuel) with confidence, leading to deeper understanding of physical and chemical unit processes taking place during the phenomena under investigation. In recent years, the authors have investigated [25-33] the dynamic behavior of diffusion flames, internal flame structure, including radical transport and reactions, extinction processes, blowoff/liftoff phenomena, and physical and chemical flame suppression processes. The objectives of the present study are to understand the physical and chemical processes of cup-burner flame suppression and to provide rigorous testing of numerical models, which include detailed chemistry and radiation sub-models.

EXPERIMENTAL PROCEDURES

The cup burner, described previously [6], consists of a cylindrical glass cup (28 mm diameter, burner rim chamfered inside) positioned inside a glass chimney (8.5 cm or 9.5 cm diameter, 53.3 cm height). To provide uniform flow, 6 mm glass beads fill the base of the chimney, and 3 mm glass beads (with two 15.8 mesh/cm screens on top) fill the fuel cup. Gas flows were measured by mass flow controllers (Sierra 860¹) which were calibrated so that their uncertainty is 2 % of indicated flow. The burner rim temperature, measured at 3.7 mm below the

¹ Certain commercial equipment, instruments, or materials are identified in this paper to adequately specify the procedure. Such identification does not imply recommendation or endorsement by NIST, nor does it imply that the materials or equipment are necessarily the best available for the intended use.

exit using a surface temperature probe after running the burner for ~10 minutes, was (514 ± 10) K.

The fuel gas used is methane (Matheson UHP, 99.9 %), and the agents are CO₂ (Airgas) and CF₃H (Dupont). The air is house compressed air (filtered and dried) which is additionally cleaned by passing it through an 0.01 μm filter, a carbon filter, and a desiccant bed to remove small aerosols, organic vapors, and water vapor. For the constant oxygen concentration method, the oxidizer fluid is made by mixing oxygen (MG Industries, 99.99 %) and nitrogen (boil-off).

To determine the suppression condition, for a fixed methane flow rate (0.34 L/min which converts to the mean fuel velocity of 0.92 cm/s), the agent was added (in increments of < 1 % near extinction) to co-flowing air (held at a constant flow rate) until extinguishment occurred (the standard cup-burner test method [1]). In this method, the oxygen concentration in the oxidizer flow decreases as the agent replaces the air. Alternatively, additional tests were conducted by replacing the nitrogen in coflowing air at a constant velocity (the constant oxygen concentration [20.9 %] method). The test was repeated at least three times at different mean coflow velocities.

An uncertainty analysis was performed, consisting of calculation of individual uncertainty components and root mean square summation of components. All uncertainties are reported as *expanded uncertainties*: $X \pm ku_c$, from a combined standard uncertainty (estimated standard deviation) u_c , and a coverage factor $k = 2$. Likewise, when reported, the relative uncertainty is ku_c / X . The expanded relative uncertainties for the experimentally determined quantities in this study are: CO₂ and CF₃H volume fractions, 4 % and 7 %, respectively.

NUMERICAL METHODS

A time-dependent, axisymmetric numerical code (UNICORN [34]) is used for the simulation of unsteady jet diffusion flames stabilized on the cup burner. The code solves the axial and radial (z and r) full Navier-Stokes momentum equations, continuity, and enthalpy- and species-conservation equations on a staggered-grid system. The body-force term due to the gravitational field is included in the axial-momentum equation to simulate upward-oriented flames. A clustered mesh system is employed to trace the gradients in flow variables near the flame surface. A detailed reaction mechanism of GRI-V1.2 [35] for methane-oxygen combustion (31 species and 346 elementary reactions) and NIST CKMech [36] for fluoromethane inhibition reactions (82 species and 1510 elementary reactions) are incorporated into UNICORN. Thermophysical properties of species are calculated from the polynomial curve fits for 300 - 5000 K. Mixture viscosity and thermal conductivity are then estimated using the Wilke and Kee expressions, respectively. A simple radiative heat-loss model [37] based on optically thin-media assumption and Plank-mean absorption coefficients for CH₄, CO, CO₂, and H₂O was incorporated into the energy equation.

The finite-difference forms of the momentum equations are obtained using an implicit QUICKEST scheme [38], and those of the species and energy equations are obtained using a hybrid scheme of upwind and central differencing. At every time-step, the pressure field is accurately calculated by solving all the pressure Poisson equations simultaneously and using the LU (Lower and Upper diagonal) matrix-decomposition technique.

Unsteady axisymmetric calculations for the cup-burner flames are made on a physical domain of 200 x 47.5 mm using a 251 × 101 (for CO₂ or CF₃H) or 541 × 251 (for CO₂ only) non-uniform grid system that yielded 0.2-mm or 0.05-mm minimum grid spacing, respectively,

in both the z and r directions in the flame zone. The computational domain is bounded by the axis of symmetry and a chimney wall boundary in the radial direction and by the inflow and outflow boundaries in the axial direction. The boundary conditions are treated in the same way as those reported in earlier papers [38, 26]. The outflow boundary in z direction is located sufficiently far from the burner exit (~ 7.5 fuel cup diameters) such that propagation of boundary-induced disturbances into the region of interest is minimal. Flat velocity profiles are imposed at the fuel and air inflow boundaries, while an extrapolation procedure with weighted zero- and first-order terms is used to estimate the flow variables at the outflow boundary. The fuel cup wall is treated as a 1-mm long and 1-mm thick tube with the temperature set at 600 K, which is somewhat higher than the afore-mentioned measurement made below the exit.

RESULTS AND DISCUSSION

Figure 1 shows a video image of a stable cup-burner flame of methane in coflowing air. The blue flame base anchored at the burner rim, and the downstream portion of the flame contracted inwardly with an orange-yellow tip due to soot formation. The flame was dynamic due to flickering. The flickering frequency measured at ~ 5 cm above the burner by a photodiode was typically ~ 11 Hz or ~ 15 Hz, depending on the air velocity. As CO_2 was added into coflowing air, the entire flame turned blue. As the CO_2 concentration approached to the suppression limit, the flame base oscillated just before the flame blew off.

Figure 2 shows the critical agent volume fraction in the oxidizer at suppression. For both cases of CO_2 and CF_3H replacing the coflowing air, the critical values were independent of the oxidizer velocity over an entire velocity range varied. This insensitivity of the suppression limit to the



Figure 1 A video image of a methane cup-burner flame in air. $U_{\text{CH}_4} = 0.92$ cm/s, $U_{\text{ox}} = 10.7$ cm/s.

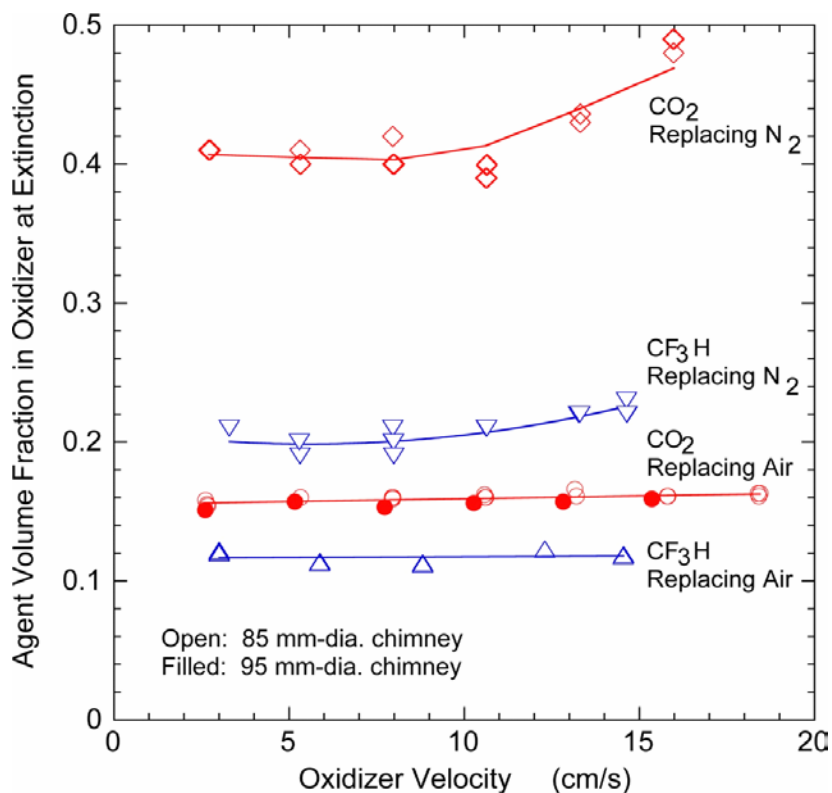


Figure 2 Effects of the oxidizer velocity on the suppression limits of methane cup-burner flames using CO_2 and CF_3H based on the standard method (replacing air) and the constant oxygen concentration method (replacing N_2).

oxidizer flow, once a minimum flow is achieved, in a so-called “plateau region” has been reported in the literature [1, 5, 9]. The fuel velocity, the fuel cup diameter, and the chimney diameter are also known to have a small or negligible impact on the agent concentration at suppression [5]. For both cases of CO₂ and CF₃H replacing the nitrogen in the oxidizer, the

plateau regions were narrower, and the critical agent concentration increased gradually with the velocity (>12 cm/s). Table 1 lists the extinguishing volume fractions of each agent determined from the plateau region, the limiting oxygen volume fractions converted from the extinguishing volume fractions ($X_{O_2} = 0.2093[1 - X_{agent}]$ where X_{O_2} = the oxygen volume fraction and X_{agent} = the agent volume fraction) for the standard method, and the adiabatic flame temperature [39] at the indicated extinguishing concentration. The measured methane flame extinguishing concentration for CF₃H by the standard method is reasonably consistent with previously reported cup-burner (11.0 % [11]) and counterflow diffusion flame results (11 % [17]) in the literature.

The agent CF₃H has been shown to decompose to HF, and COF₂, when added to both premixed and co-flow diffusion flames of methane and air [6]. Hence, the equilibrium composition [39] at the adiabatic flame temperature in Table 1 includes HF, CO₂, at much lesser amount (replacing N₂ case only), COF₂, and F. As shown, the final temperature is not much different than that for an uninhibited methane-air flame (2132 K). The higher flame temperatures at suppression for CF₃H illustrate its chemical inhibition effects compared to physically acting CO₂.

Numerical simulations have been performed to investigate the flame structure of methane flames with CO₂ [31, 32], CF₃H, and

Table 1 Extinguishing Agent Volume Fractions and Limiting Oxygen Volume Fractions

Agent	Extinguishing Agent Volume Fraction (%)	Limiting O ₂ Volume Fraction (%)	Adiabatic Flame Temperature (K)
Replacing Air			
CO ₂	15.9 ± 0.6	17.6 ± 0.1	1926
CF ₃ H	11.7 ± 0.8	18.5 ± 0.2	2109
Replacing N ₂			
CO ₂	40.2 ± 2.0	N/A	1963
CF ₃ H	20.3 ± 1.5	N/A	2020

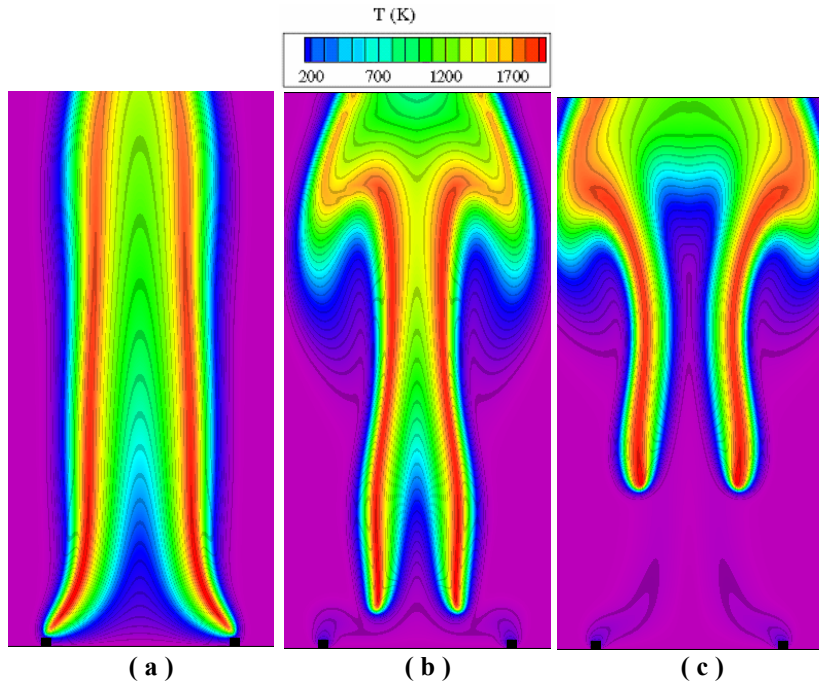


Figure 3 Calculated temperature field in methane cup-burner flames in agent laden coflowing air. $U_{CH_4} = 0.92$ cm/s, $U_{ox} = 10.7$ cm/s. (a) $X_{CO_2} = 0.05$, (b) $X_{CO_2} = 0.145$, (c) $X_{CF_3H} = 0.101$.

CO₂/Fe(CO)₅ [33] added to co-flowing air. Figure 3 shows snapshots of the calculated temperature field for fully dynamic flames with a CO₂ volume fraction of 0.05 and 0.145 (the suppression limit), and a CF₃H volume fraction of 0.101 (the suppression limit). The calculated critical agent volume fractions at suppression were ~9 % lower than the measured values listed in Table 1. Considering the complexity in the physico-chemical processes involved in the suppression condition, the predicted results are in reasonably good agreements. For $X_{\text{CO}_2} = 0.05$ (Fig. 3a), the flame base was attached to the burner rim. At the suppression limit (Fig. 3b), the flame base detached from the burner rim inwardly, drifted downstream, and eventually blew off. For $X_{\text{CF}_3\text{H}} = 0.101$ (Fig. 3a), a series of events was the same as for the CO₂ case. The computation has revealed that the suppression of cup-burner flames occurs via a blowoff process (in which the flame base drifts downstream) rather than the global extinction phenomenon typical of counterflow diffusion flames. This result is particularly important when comparing the results for different flame configurations (cup burner vs. counterflow burner) and when

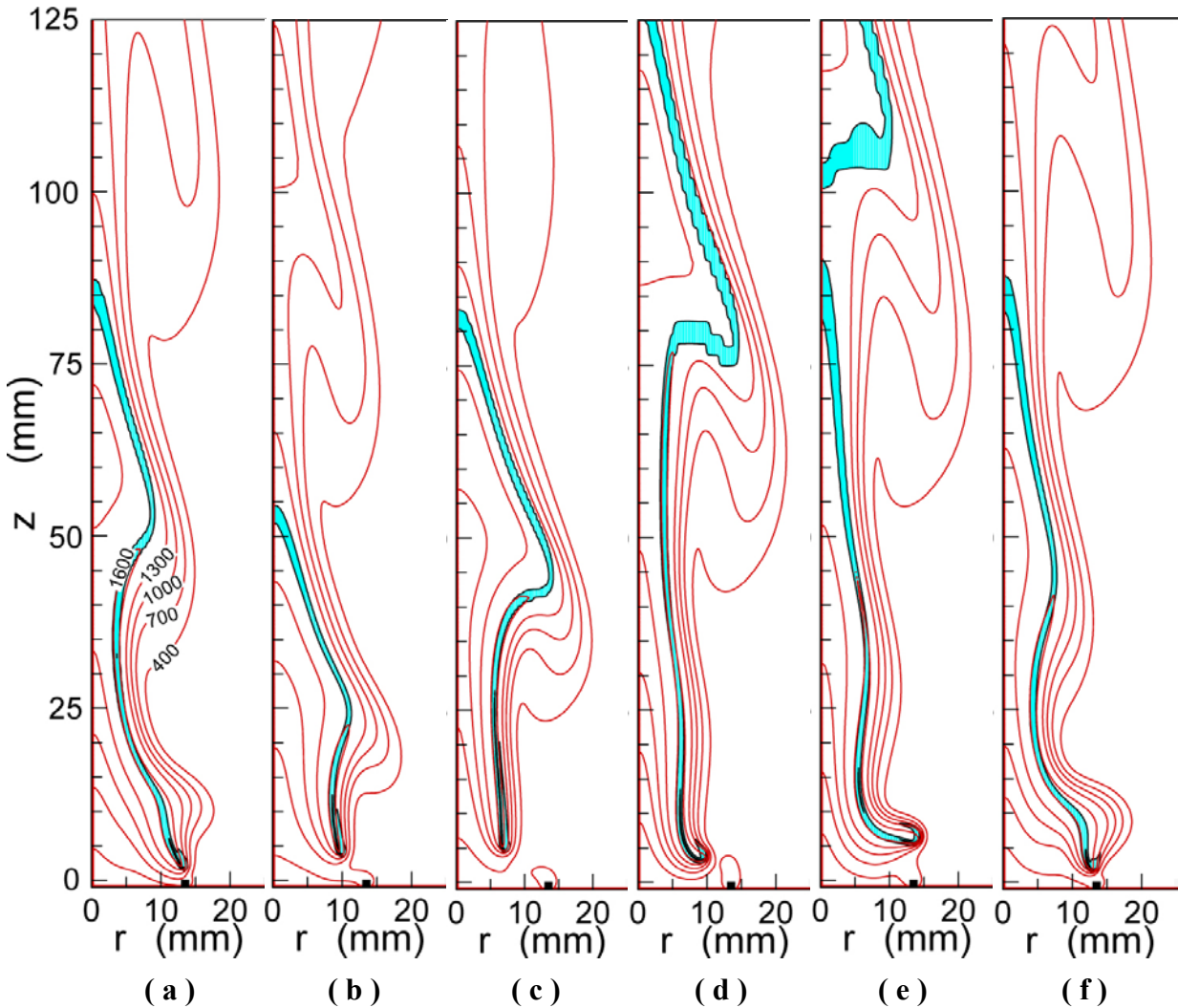


Figure 4 Calculated temperature and heat-release rate contours showing flame flickering and flame-base oscillation in a near-limit methane cup-burner flame in agent laden coflowing air. $U_{\text{CH}_4} = 0.92$ cm/s, $U_{\text{ox}} = 10.7$ cm/s, $X_{\text{CO}_2} = 0.14$. (a) $t = 0$ s, (b) 0.04 s, (c) 0.08 s, (d) 0.12 s, (e) 0.14 s, (f) 0.16 s.

considering fire suppression strategies.

The flame flickering and the flame-base oscillation, observed just before flame blew off by adding CO_2 , were also captured in numerical simulations. Figure 4 shows a time sequence of the calculated isotherms and heat-release rate contours in a dynamic near-limit methane cup-burner flame with $X_{\text{CO}_2} = 0.14$. The generation and evolution of buoyancy-induced vortices in the near field resulted in wavy isotherms and the flame zone visualized as the high heat-release zone. The calculated flame flickering frequency was ~ 11 Hz (which corresponded to a period of 0.909 s). Thus, the flame in Fig. 4 underwent nearly two cycles of the buoyancy-induced vortex generation, during which the flame base traveled a cycle of oscillation. Thus, the flame-base oscillating frequency is half the flame flickering frequency. Interestingly, the flame tip separation also occurred at half the flickering frequency because the vortex generated when the flame base was innermost position was weak and did not develop enough to separate the bulk of the fuel to form a separated flame island.

To investigate detailed mechanisms of the flame-base oscillation prior to suppression, Figure 5 shows selected replots of Fig. 4 in the flame stabilizing region. As was reported in earlier papers [25-29], the reaction kernel (a peak reactivity spot) formed in the flame base stabilizes the trailing diffusion flame downstream. Because of a high CO_2 concentration near the suppression limit, the reaction rates were reduced, and therefore, the flame base was susceptible to small velocity fluctuations. As a vortex was generated outside the flame zone near the burner exit, the velocity of entrainment flow into the flame base increased, thus pushing the flame zone inwardly (Fig. 5a). As the flame base reached the innermost position, a large fuel-air mixing space was formed; and because the bulk of hot vortex passed downstream, the buoyancy-driven entrainment velocity into the flame base decreased (Fig. 5b). Then the flame base propagated back outwardly, pushing the mixture ahead of the flame base (Fig. 5c); here, the reaction kernel structure resembled that of a propagating flame through a mixing layer formed in a fuel jet [30]. As the flame base consumed the mixture and reached the burner radius, it turned downward toward the burner rim (Fig. 5d), returning to the attached flame position (Fig. 5a). Therefore, the flame-base oscillation is linked to the buoyancy-induced vortex generation and, in turn, the flame flickering process. As the CO_2 concentration was increased to the suppression limit, the flame base became weaker and could not come back from the innermost position, thereby drifting upward to blow off.

CONCLUSIONS

The suppression limits and oscillatory behaviors of cup-burner diffusion flames of methane have been studied under normal gravity. The measured extinguishing agent volume fractions by the standard method (replacing air) are: CO_2 , (15.9 ± 0.6) % and CF_3H , (11.7 ± 0.8) %; and those by the constant oxygen concentration method (replacing N_2) are: CO_2 , (40.2 ± 2.0) % and CF_3H , (20.3 ± 1.5) %. The suppression of cup-burner flames occurs via a blowoff process rather than the global extinction phenomenon typical of counterflow diffusion flames. The axisymmetric flame-base oscillation is observed sporadically prior to blowoff. The cup-burner flame flickering frequency depends on the coflowing air velocity and exhibits a mode transition between ~ 11 Hz and ~ 15 Hz. The time-dependent direct numerical simulation with detailed chemistry has predicted the suppression limits for both agents in the standard method with a good agreement with the measurement, captured the flame flickering mode at ~ 11 Hz, and revealed the flame base oscillation occurred at half the flickering frequency.

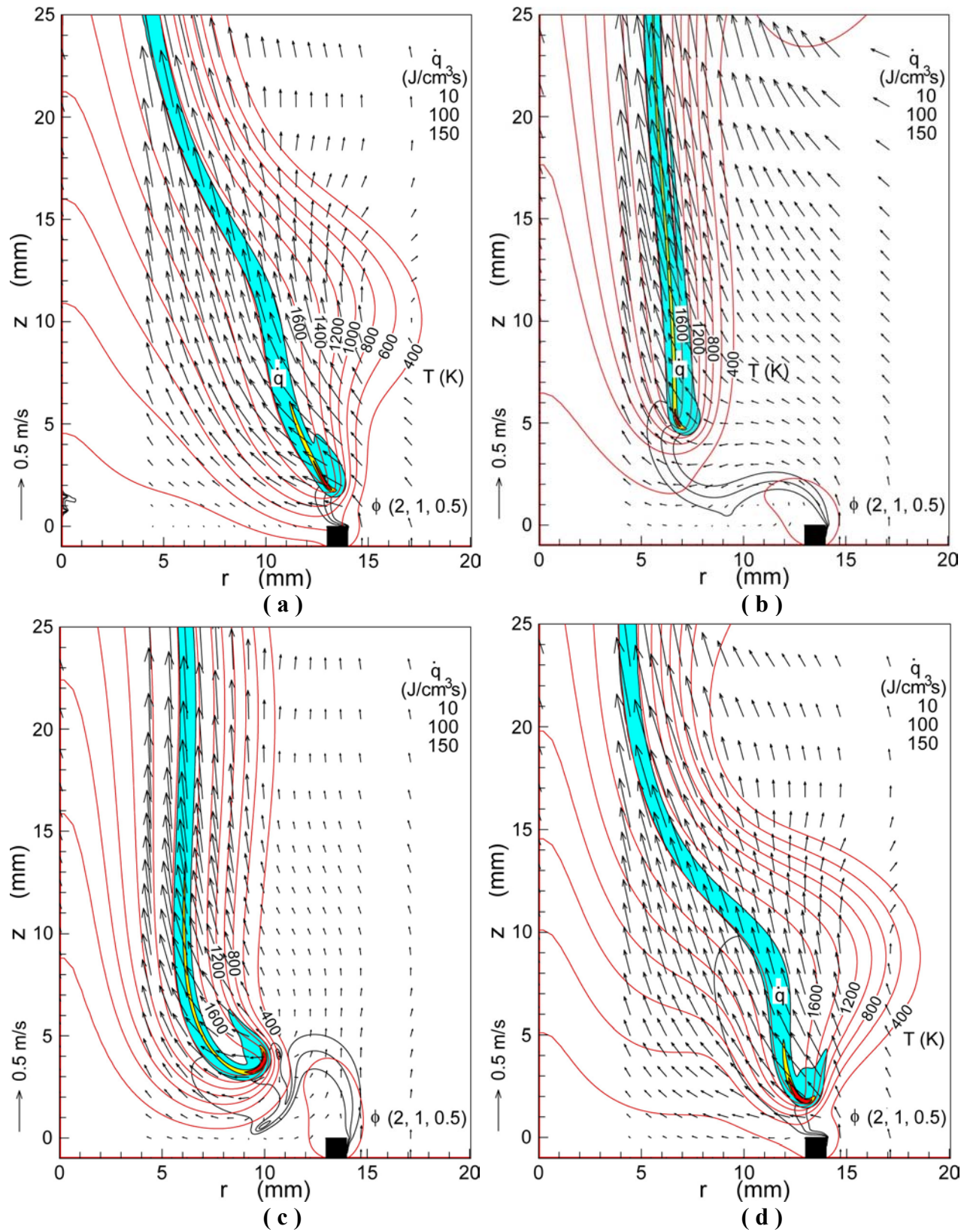


Figure 5 Calculated structure of an oscillating near-limit methane cup-burner flame in agent laden coflowing air. $U_{CH_4} = 0.92$ cm/s, $U_{ox} = 10.7$ cm/s, $X_{CO_2} = 0.14$. (a) $t = 0$ s, (b) 0.08 s, (c) 0.12 s, (d) 0.16 s.

ACKNOWLEDGMENT

This research was supported by the Office of Biological and Physical Research, NASA, Washington, D.C.

REFERENCES

1. National Fire Protection Agency, *Standard on Clean Agent Fire Extinguishing Systems*, NFPA 2001, 1994.
2. Bajpai, S. N., An Investigation of the Extinction of Diffusion Flames by Halons, *Journal of Fire and Flammability*, 5, 255 (1974).
3. Hirst, R., and Booth, K., Measurements of Flame-Extinguishing Concentrations, *Fire Technology*, 13, 4 (1977).
4. Sheinson, R. S., Pender-Hahn, J. E., and Indritz, D., The Physical and Chemical Action of Fire Suppressants, *Fire Safety Journal*, 15, 437-450 (1989).
5. Hamins, A., Gmurczyk, G., Grosshandler, W., Rehwoldt, R. G., Vazquez, I., Cleary, T., Presser, C., and Seshadri, K., Flame Suppression Effectiveness, *Evaluation of Alternative In-Flight Fire Suppressants for Full-Scale Testing in Simulated Aircraft Engine Nacelles and Dry Bays* (W. L. Grosshandler, R. G. Gann, and W. M. Pitts, Eds.), National Institute of Standards and Technology, NIST SP 861, 1994, pp. 345-465.
6. Linteris, G.T. and Gmurczyk, G.W., in *Fire Suppression System Performance of Alternative Agents in Aircraft Engine and Dry Bay Laboratory Simulations* (R.G. Gann, Ed.), National Institute of Standards and Technology, NIST SP 890, Gaithersburg, MD, 1995, pp. 201-318.
7. Sakai, R., Saito, N., Saso, Y., Ogawa, Y., and Inoue, Y., Flame Extinguishing Concentrations of Halon Replacements for Flammable Liquids, Report of Fire Research Institute of Japan, No. 80, 1995, pp. 36-42.
8. Moore, T. A., Weitz, C. A., and Tapscott, R. E., An update of NMERI Cup-Burner Test Results, Proceedings of the 6th Halon Options Technical Working Conference (HOTWC-96), Albuquerque, NM, 1996, pp. 551-564.
9. Moore, T. A., Martinez, A., and Tapscott, R. E., A Comparison of the NMERI and ICI-style Cup-Burners, Proceedings of the 7th Halon Options Technical Working Conference (HOTWC-97), Albuquerque, NM, 1997, pp. 388-395.
10. Saito, N., Ogawa, Y., Saso, Y., and Sakai, R., Improvement on Reproducibility of Flame Extinguishing Concentration Measured by Cup Burner Method, Report of Fire Research Institute of Japan, No. 81, 1996, pp. 22-29.
11. Senecal, J. A., Cup-burner Extinguishing Concentration Correlation with C₁-C₈ class B fuel properties, Proceedings of the 8th Halon Options Technical Working Conference (HOTWC-98), Albuquerque, NM, 1998, pp. 70-79.
12. Babb, M., Gollahalli, S. R., and Sliepcevich, C. M., Extinguishment of Liquid Heptane and Gaseous Propane Diffusion Flames, *Journal of Propulsion and Power*, 15, 260-265 (1999).
13. Tsuji, H., Counter flow diffusion flames. *Progress in Energy and Combust. Sci.*, 8, 93-119 (1982).
14. Simmons, R. F., and Wolfhard, H. G., Some Limiting Oxygen Concentrations for Diffusion Flames in Air Diluted with Nitrogen, *Combustion and Flame*, 1, 155-161 (1957).
15. Hamins, A., Trees, D., Seshadri, K., and Chelliah, H. K., Extinction of Nonpremixed Flames with Halogenated Fire Suppressants, *Combustion and Flame*, 99, 221-230 (1994).
16. Saso, Y., Saito, N., Liao, C., and Ogawa, Y., Extinction of Counterflow Diffusion Flames with Halon Replacements, *Fire Safety Journal*, 26, 303-326 (1996).
17. Papas, P., Fleming, J. W., and Sheinson, R. S., Extinction of Non-premixed Methane- and Propane-Air Counterflow Flames Inhibited with CF₄, CF₃H and CF₃Br, *Proceedings of The Combustion Institute*, Vol. 26, 1996, pp. 1405-1411.
18. Pitts, W. M., and Blevins, L. G., An Investigation of Extinguishment by Thermal Agents using Detailed Chemical Modeling of Opposed-flow Diffusion Flames, Proceedings of the 9th Halon Options Technical Working Conference (HOTWC-99), Albuquerque, NM, 1999, pp. 145-156.
19. Takahashi, F., Schmoll, W. J., Strader, E. A., and Belovich, V. M., Suppression of a Nonpremixed Flame Stabilized by a Backward-Facing Step, *Combustion and Flame*, 122, 105-116 (2000).
20. Friedman, R., Fire Safety in Extraterrestrial Environments, NASA/TM-1998-207417, 1998.

21. Friedman, R., and Ross, H. D., Combustion Technology and Fire Safety for Human-crew Space Missions, In *Microgravity Combustion: Fire in Free Fall* (H. D. Ross Ed.), Academic Press, San Diego, 2001, p.83.
22. Grosshandler, W. L., Gann, R. G., and Pitts, W. M., (eds.), Evaluation of Alternative In-Flight Fire Suppressants for Full-Scale Testing in Simulated Aircraft Engine Nacelles and Dry Bay, SP 861, National Institute of Standards and Technology, 1994.
23. Harrison, G. C., Halon Replacement in Aircraft and Industrial Applications, In *Halon Replacements: Technology and Science* (A. W. Miziolec and W. Tsang, Eds.), American Chemical Society, Washington, DC, 1995, pp. 74-84.
24. Annon., Workshop on Research for Space Exploration: Physical Sciences and Process Technology, NASA/CP-1998-207431, May 1998.
25. Takahashi, F., Schmoll, W. J., and Katta, V. R., Attachment Mechanisms of Diffusion Flames, *Proceedings of The Combustion Institute*, Vol. 27, 1998, pp. 675-684.
26. Takahashi, F., and Katta, V. R., Chemical Kinetic Structure of the Reaction Kernel of Methane Jet Diffusion Flames, *Combustion Science and Technology*, 155: 243-279 (2000).
27. Takahashi, F., and Katta, V. R., A Reaction Kernel Hypothesis for the Stability Limit of Methane Jet Diffusion Flames, *Proceedings of The Combustion Institute*, Vol. 28, 2000, pp. 2071-2078.
28. Takahashi, F., and Katta, V. R., A Numerical and Experimental Study of The Structure of a Diffusion Flame Established in A Laminar Boundary Layer Along a Vertical Porous Plate, Proceedings of the Third International Symposium on Scale Modeling, Nagoya, Japan, 2000.
29. Takahashi, F., and Katta, V. R., Reaction Kernel Structure and Stabilizing Mechanisms of Jet Diffusion Flames in Microgravity, *Proceedings of The Combustion Institute*, Vol. 29, 2002, pp. 2509-2518.
30. Takahashi, F., and Katta, V. R., Propagation and Structure of Edge Diffusion Flames in Axisymmetric Hydrocarbon Fuel Jets, 19th International Colloquium on The Dynamics of Explosions and Reactive Systems (ICDERS), Hakone, Japan, July 2003.
31. Katta, V. R., Takahashi, F., and Linteris, G. T., Numerical Investigations of CO₂ as Fire Suppressing Agent, *Fire Safety Science: Proceedings of the Seventh International Symposium*, International Association for Fire Safety Science, 2002, in press.
32. Katta, V. R., Takahashi, F., and Linteris, G. T., Extinction Characteristics of Cup-Burner Flame in Microgravity, 41st Aerospace Sciences Meeting and Exhibit, AIAA Paper No. 2003-1150, Reno, NV, 2003.
33. Linteris, G. T., Katta, V. R., and Takahashi, F., Experimental and Numerical Evaluation of Metallic Compounds for Suppressing Cup-Burner Flames, *Combustion and Flame*, submitted (2003).
34. Roquemore, W. M., and Katta, V. R., Role of Flow Visualization in the Development of UNICORN, *Journal of Visualization*, Vol. 2, No. 3/4, 257-272 (2000).
35. Frenklach, M., Wang, H., Goldenberg, M., Smith, G. P., Golden, D. M., Bowman, C. T., Hanson, R., K., Gardiner, W. C., and Lissianski, V., GRI-Mech—An Optimized Detailed Chemical Reaction Mechanism for Methane Combustion, Technical Report No. GRI-95/0058, Gas Research Institute, Chicago, Illinois, 1995.
36. Anon., NIST CKMech (Thermochemistry, Kinetics, Mechanisms), <http://fluid.nist.gov/ckmech.html>.
37. Annon., Computational Submodels, International Workshop on Measurement and Computation of Turbulent Nonpremixed Flames., <http://www.ca.sandia.gov/tdf/Workshop/Submodels.html>, 2001.
38. Katta, V. R., Goss, L. P., and Roquemore, W. M., Numerical Investigations of Transitional H₂/N₂ Jet Diffusion Flames, *AIAA Journal*, 32, 84 (1994).
39. McBride, B. J., and Gordon, S., Computer Program for Calculation of Complex Chemical Equilibrium Compositions and Applications—II. Users Manual and Program Description, NASA Reference Publication 1311, June 1996.